*Original Article*

# Diagnostic Performance of Multidetector Computed Tomography [MDCT] for Differentiating between Pancreatic Adenocarcinoma and Non-Benign Pancreatic Neuroendocrine Tumor

Sopa Pongpornsup MD[1], Janejira Chumcheon MD[1], Aphinya Charoensak MD[1]

[1] Division of Diagnostic Radiology, Department of Radiology, Faculty of Medicine Siriraj Hospital, Mahidol University, Bangkok, Thailand

***Objective:*** To evaluate the accuracy, sensitivity, and specificity of various abdominal computed tomography [CT] features in differentiating between pancreatic adenocarcinoma [PAC] and non-benign pancreatic neuroendocrine tumor [nPET].

***Materials and Methods:*** Sixty-seven patients with pathologically confirmed PAC (n = 49) and nPET (n = 18) who had undergone preoperative abdominal CT were enrolled for this retrospective review. Imaging features on abdominal CT were analyzed. Sensitivity, specificity, positive, and negative predictive value of each significant variable (*p*-value of less than 0.05) were calculated.

***Results:*** Tumor location, demarcation, calcification, vascularity, bile duct dilatation, liver metastasis, adjacent organ invasion, and lymphadenopathies, were CT features for distinguish between the two groups in the univariate analysis. Tumor attenuation values on non-contrast, arterial phase, and portal venous phase [PVP], and tumor-to-pancreas contrast during arterial and PV phases of PAC were significantly lower than of nPET. In the multivariate analysis, an ill-defined margin, hypo/isovascularity, and absence of liver metastasis, were indicative of PAC than nPET.

***Conclusion:*** Abdominal CT is the reliable method to differentiate between PAC and nPET.

***Keywords:*** Pancreas, Pancreatic adenocarcinoma, Non-benign pancreatic neuroendocrine tumor, Abdominal computed tomography

**J Med Assoc Thai 2018; 101 (2): 239-47**
**Website:** http://www.jmatonline.com

Pancreatic cancer is an aggressive cancer and has poor prognosis. It was the fourth cause of cancer-related deaths in the United States in 2016 with only 8% of the 5-year relative survival[1]. Furthermore, more than 60% of all new cases of pancreatic cancer are diagnosed at advanced stage in Thailand[2].

Solid pancreatic neoplasms can be classified into several groups according to their originated cells, which pancreatic adenocarcinoma [PAC] is the most common pancreatic tumors, accounts for 85% to 95%, and pancreatic neuroendocrine tumor [PET] is the second, at approximately 1% to 5%[3]. According to the difference of their behavior, prognosis, and treatment strategy between PAC and PET, discrimination of these tumors is necessary[3,4]. Tumor marker levels are difficult in differentiating pancreatic tumors, including PAC and PET. In addition, tissue diagnosis is an invasive procedure. Therefore, computed tomography [CT] is a useful non-invasive modality.

Previous studies have shown the differentiation of PET from PAC based on its typical features on CT imaging[4]. However, differentiating between PAC and non-benign PET [nPET] based on CT imaging is not well known and remains challenging. For these reasons, the authors investigated the different CT imaging to find the features between PAC and nPET that might be helpful in making diagnosis.

**Correspondence to:**

Pongpornsup S. Department of Radiology, Faculty of Medicine, Siriraj Hospital, 2 Wang Lang Road, Bangkoknoi, Bangkok 10700, Thailand.
**Phone**: +66-2-4199039, **Fax**: +66-2-4127785
**Email**: sopa2108@hotmail.com

## Materials and Methods

### *Sample size calculation*

The present study was a comparison study between two groups, which the formula is two proportions independent. According to the study conducted by Low et al[3], calcification in adeno-carcinoma was found to be 2% (P1 = 0.02) and neuro-endocrine 20% (P2 = 0.2). At type 1 and 2 errors of 0.05 and 0.2, the studies are required for each group to be 47 subjects.

$$n/gr = \left(\frac{Z_\alpha\sqrt{2P(1-P)} + Z_\beta\sqrt{P_1(1-P_1) + P_2(1-P_2)}}{P_1-P_2}\right)^2$$

**How to cite this article**: Pongpornsup S, Chumcheon J, Charoensak A. Diagnostic performance of multidetector computed tomography [MDCT] for differentiating between pancreatic adenocarcinoma and non-benign pancreatic neuroendocrine tumor. J Med Assoc Thai 2018;101:239-47.

where

Z = values derived from the standard normal distribution table. When defining type 1 error (α) is equal to 0.05, then Z is 1.96, and when the type 2 error (β) is 0.2, then Z is equal to 0.842

P1 = calcification in PAC was 2% (P1 = 0.02)

P2 = calcification in PET was 20% (P1 = 0.2)

### *Patient population*

The Institutional Review Board approved the present study and the informed consent of patients was waived because of the retrospective review of clinical and imaging data. The authors reviewed the medical patient records at Siriraj Hospital between January 2007 and December 2014 by using a computerized search for patients diagnosed as pancreatic neoplasms from International Classification of Diseases Tenth Revision [ICD-10]. The inclusion criteria were 1) patients with pathologically confirmed PAC or PET through surgery or biopsy, except PAC that developed from intraductal papillary mucinous neoplasm [IPMN], 2) patients that underwent enhanced abdominal CT scans according to the institution's routine protocol prior to the pathologic diagnosis, and 3) absence of a history of surgery or interventional treatment in pancreas before the CT examination. Five from 54 patients with PAC were subsequently excluded because two had other primary intraabdominal cancers and three could not be evaluated for the exact intrapancreatic lesions. Thirty-one patients with PET were identified. According to the World Health Organization Classification of Neuroendocrine Tumors, PET can be classified in two main groups, benign PET and nPET, by using the histologic features, tumor grading, tumor size, Ki-67 index, presence of angioinvasion, adjacent organ invasion, and metastasis[5,6]. The nPET should show at least one of the following features, size of 2 cm or larger, Ki-67 index of more than 2%, presence of angioinvasion, adjacent organ invasion, and metastases. Consequently, thirteen patients were excluded from the present study as their symptoms corresponded with benign PET. Finally, 49 patients with PAC and 18 patients with nPET were included in the present study.

### *Clinical data collection*

For all patients, the medical records were retrospectively reviewed for demographic data, associated syndromes, and serum tumor marker levels prior to surgery or tissue biopsy (carbohydrateantigen 19-9 [CA 19-9], carcinoembryonic antigen [CEA], and alpha-fetoprotein [AFP]).

### *Computed tomography imaging*

All abdominal CT scans were performed by using the 64 sliced multidetector computed tomography [MDCT] machines (GE light speed 64 VCT scanner at 1.25 mm slice thickness or GE Discovery CT 750 HD scanner at 1.25 mm slice thickness or Siemens Somaton definition scanner at 1.5 mm slice thickness). The exposures parameters were 120 kVp and 250 to 300 mAs. The CT coverage was performed from hepatic dome to iliac crests in CT scan of upper abdomen, or from hepatic dome to pubic symphysis in CT scan of whole abdomen, in supine position on both non-contrast phase and post-contrast phase. To obtain luminal distension of stomach and small bowel loops, and to reduce bowel gas artifact, water was routinely used as a negative oral contrast agent[7]. For CT scan of upper abdomen, 750 ml of water was administrated 30 minutes before scanning as follows, 250 ml of water every 15 minutes with the last 250 ml immediately before scanning. There was a slight difference in CT scan of whole abdomen when 500 ml of water and 500 ml of oral contrast medium were ingested 30 minutes before scanning. Rectal water was also used as patient could tolerate in CT scan of whole abdomen. Non-ionic iodinated contrast material was calculated at 2 ml/kg body weight plus water 20 ml and was administered intravenously with injected rate at about 3 ml/second by injector and delayed scan after intravenous contrast administration at 35 seconds for arterial phase, 40 seconds for pancreatic phase, 80 seconds for portal venous phase [PVP], and 5 minutes for delayed phase.

### *Image analysis*

All CT images were reviewed by two abdominal radiologists in consensus from a picture archiving and communication system workstation. Both observers were aware of the alternative diagnoses of PAC or nPET but were blinded to the clinical and histopathologic results in each case.

### *Qualitative analysis*

Qualitative analysis including morphologic features, enhancement features, and associated findings were evaluated.

For comparison of the morphologic features between PAC and nPET, the following features were evaluated, a) tumor size, b) location (head/uncinate/neck versus body/tail/diffuse), c) demarcation (ill-defined versus well-defined), d) appearance (solid versus cystic), e) presence of necrosis, and f) presence of calcification.

For comparison of the enhancement features, the following features were evaluated, a) pattern enhancement (homogeneous versus heterogeneous), and b) vascularity (hypo/isovascular versus hypervascular). The vascularity of the lesions was determined by comparing attenuation of the lesion on each dynamic phase with the adjacent pancreatic parenchyma.

For the associated findings, the following features were evaluated, a) presence of adjacent vessels invasion (adjacent arteries including celiac artery, small mesenteric artery [SMA]), and hepatic artery, adjacent veins including small mesenteric vein [SMV], portal vein, and splenic vein), b) presence of bile duct dilatation (main pancreatic duct and common bile duct [CBD]), c) presence of distal pancreatic parenchymal atrophy, d) presence of metastases (liver and peritoneum), e) presence of adjacent organs invasion, and f) presence of intraabdominal lymphadenopathies. Vascular invasion was defined as tumor-to-vessel contiguity greater than 50%, tear drop sign of SMV, vessel deformity, irregularity of vessel wall, luminal narrowing, presence of thrombosis or vessel occlusion[8,9]. For nodal invasion, a short-axis diameter of greater than 10 mm, ovoid shape, clustering of nodes, or the absence of a fatty hilum were used as criteria[10].

### *Semiquantitative analysis*

For quantitative analysis, lesion size, tumor attenuation values (on non-contrast, arterial, pancreatic, portal venous, and delayed phases), and tumor-to-pancreas contrast on each phase were evaluated. For measurement of tumor attenuation values, the region of interest [ROI] was drawn on each phase at the pancreatic lesion, avoiding necrotic and cystic areas. Tumor-to-pancreas contrast was calculated using the attenuation differences between the tumor and pancreatic parenchyma on each phase.

### *Statistical analysis*

Levels of inter-observer agreement were assessed using Cohen's kappa statistics, 0.81 to 1 as almost perfect agreement, 0.61 to 0.8 as substantial agreement, 0.41 to 0.6 as moderate agreement, 0.21 to 0.4 as fair agreement, 0.01 to 0.2 as slight agreement, and 0 or less as poor agreement, as defined in a study by Landis and Koch[11]. All the nominal variants were compared using the Chi-square test or Fisher's exact test, as appropriate. The t-test or Mann-Whitney test was performed for continuous variables. In ROC analysis, the appropriate cutoff value of tumor attenuation on non-contrast and portal venous phases, and tumor-to-pancreas contrast during PVP corresponding to the maximal Youden index were determinate. A *p*-value of less than 0.05 were regarded as statistically significant. Then, positive predictive value [PPV], negative predictive value [NPV], sensitivity, and specificity of each significant variable were calculated. A two-sided significant level of 5% was considered to indicate statistical significance for all analyses. All statistical analyses were performed using the SPSS 18.0 software package (SPSS Inc., Chicago, IL).

## Results

### *Inter-observer agreement*

The inter-observer agreement was moderate to good for all items except appearance of lesion. Further details are presented in Table 1.

### *Clinical and pathological characteristics*

The mean age, sex, associated syndrome, and tumor markers with PAC and nPET are shown in Table 2. The mean age and CA 19-9 levels differences between the two groups were significant with higher

**Table 1.** Inter-observer agreement in each CT finding

| CT findings | Inter-observer agreement* |
|---|---|
| Location | 0.86 |
| Demarcation | 0.67 |
| Appearance | 0.31 |
| Presence of necrosis | 0.72 |
| Presence of calcification | 0.80 |
| Pattern enhancement | 0.71 |
| Vascularity | 0.89 |
| Invasion of adjacent vessels | |
| Celiac artery | 1.00 |
| SMA | 1.00 |
| Hepatic artery | 0.92 |
| SMV | 0.58 |
| Portal vein | 0.71 |
| Splenic vein | 0.88 |
| Bile duct dilatation | |
| Main pancreatic duct | 0.82 |
| CBD | 0.93 |
| Distal pancreatic parenchymal atrophy | 0.72 |
| Metastasis | |
| Liver | 0.71 |
| Peritoneal implant | 0.41 |
| Adjacent organ invasion | 0.60 |
| Presence of intraabdominal lymphadenopathies | 0.67 |

CBD = common bile duct; CT = computed tomography; SMA = small mesenteric artery; SMV = small mesenteric vein

* Cohen's kappa statistics

**Table 2.** Clinical and pathological characteristics of patients with PAC and nPET

| | PAC (n = 49) | nPET (n = 18) | *p*-value* |
|---|---|---|---|
| Age (year), mean ± SD | 64.5±10.3 | 54.9±13.2 | 0.003† |
| Gender (male/female) | 25/24 | 5/13 | 0.090 |
| Syndrome, n (%) | 0 (0.0) | 1 (5.6) | 0.269 |
| Tumor markers, median (range) | | | |
| CA 19-9 (U/ml) | 494.7 (0.6 to 44,829.0) | 22.3 (1.2 to 175.6) | 0.012† |
| CEA (ng/ml) | 3.4 (1.0 to 150.0) | 2.9 (1.0 to 10.2) | 0.255 |
| AFP (IU/ml) | 2.6 (0.8 to 131.0) | 2.6 (1.2 to 21.6) | 1.000 |

AFP = alpha-fetoprotein; CA 19-9 = carbohydrateantigen 19-9; CEA = carcinoembryonic antigen; nPET = non-benign pancreatic neuroendocrine tumor; PAC = pancreatic adenocarcinoma

* t-test, Chi-square test, or Mann-Whitney test

† Statistically significant

mean age and higher CA 19-9 level in the PAC group ($p = 0.003$ and 0.012, respectively).

### *Morphologic features, enhancement features, and associated findings*

Tumor location at head/uncinate/neck of pancreas, an ill-defined margin, absence of calcification, hypo/isovascularity, main pancreatic duct and CBD dilatation, absence of liver metastasis, presence of adjacent organ invasion, and presence of intraabdominal lymphadenopathies were significant imaging features of PAC (all, $p<0.05$). Tumor location at body/tail, well-defined margin, hypervascularity, no main pancreatic, and CBD dilatation, hepatic metastasis, and no intrabdominal adenopathy were significant imaging features of nPET (all, $p<0.05$). Detailed description of the morphologic features, enhancement features and associated findings of both groups are provided in Table 3, and representative images are shown in Figure 1-3.

### *Tumor attenuation values and tumor-to-pancreas contrast: semiquantitative analysis*

The tumor attenuation values and tumor-to-pancreas contrast of the PAC and nPET are summarized in Table 4. The differences in tumor attenuation values during non-contrast, arterial, and portal venous phases, and tumor-to-pancreas contrast during arterial and portal venous phases were significant between the two groups with lower all values in the PAC group ($p = 0.028, 0.003, <0.001, <0.001$, and $<0.001$, respectively).

Although there was substantial overlap in tumor attenuation values on non-contrast and portal venous phases, and tumor-to-pancreas contrast during PVP between two groups, the optimal cutoff point of tumor attenuation values on non-contrast and portal venous phases, and tumor-to-pancreas contrast during PVP for differentiating PAC from nPET was 40 HU, 85 HU, and 3 HU in ROC curve analysis, and the AUC was 0.650, 0.823, and 0.865, respectively (Figure 4-6). Applying these cutoff values gave the best sensitivity and specificity for diagnosis PAC. Because of small number of patients who performed CT scans during arterial phase, this variable was not included in ROC curve analysis.

Tumor vascularity showed highest sensitivity (93.9%), specificity (77.8%), PPV (92%), and NPV (82.4%) to differentiate of PAC and nPET. The ill-

**Table 3.** Morphologic features, enhancement features, and associated findings of patients with PAC and nPET

| CT findings | PAC (n = 49) | nPET (n = 18) | *p*-value* |
|---|---|---|---|
| Size (cm), mean ± SD | 34.2±23.3 | 53.9±36.4 | 0.044 |
| Location, n (%) | | | 0.001† |
| Head/uncinate/neck | 40 (81.6) | 7 (38.9) | |
| Body/tail/diffuse | 9 (18.4) | 11 (61.1) | |
| Demarcation, n (%) | | | <0.001† |
| An ill-defined | 47 (95.9) | 7 (38.9) | |
| Well-defined | 2 (4.1) | 11 (61.1) | |
| Appearance, n (%) | | | 1.000 |
| Solid | 48 (98.0) | 18 (100) | |
| Cystic | 1 (2.0) | 0 (0.0) | |
| Presence of necrosis, n (%) | 18 (36.7) | 7 (38.9) | 0.872 |
| Presence of calcification, n (%) | 8 (16.3) | 10 (55.6) | 0.004† |
| Pattern enhancement, n (%) | | | 1.000 |
| Homogeneous | 7 (14.3) | 2 (11.1) | |
| Heterogeneous | 42 (85.7) | 16 (88.9) | |
| Vascularity, n (%) | | | <0.001† |
| Hypo/isovascular | 46 (93.9) | 4 (22.2) | |
| Hypervascular | 3 (6.1) | 14 (77.8) | |
| Invasion of adjacent vessels, n (%) | | | |
| Arterial invasion | 10 (20.4) | 2 (11.1) | 0.490 |
| Venous invasion | 17 (34.7) | 9 (50.0) | 0.254 |
| Main pancreatic duct dilatation, n (%) | 38 (77.6) | 4 (22.2) | <0.001† |
| Diameter (cm), mean ± SD | 7.9±5.1 | 5.6±1.9 | 0.384 |
| CBD dilatation, n (%) | 35 (73.5) | 1 (5.6) | <0.001† |
| Diameter (cm), mean ± SD | 16.3±4.2 | 13 | |
| Presence of metastases, n (%) | | | |
| Liver metastasis | 6 (12.2) | 12 (66.7) | <0.001† |
| Peritoneal implant | 5 (10.2) | 0 (0.0) | 0.313 |
| Adjacent organ invasion, n (%) | 25 (51.0) | 3 (16.7) | 0.011† |
| Intraabdominal lymphadenopathies, n (%) | 37 (75.5) | 7 (38.9) | 0.005† |

CBD = common bile duct; nPET = non-benign pancreatic neuroendocrine tumor; PAC = pancreatic adenocarcinoma

* t-test or Chi-square test

† Statistically significant

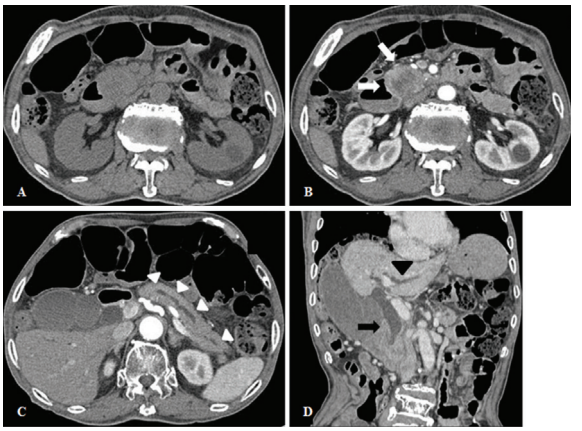

**Figure 1.** A 77-year-old man with typical pancreatic adenocarcinoma and mark elevated serum CA 19-9 level (865.0 U/ml). A: Non-contrast phase CT image in axial plane shows enlargement of pancreatic head without calcification. B, C: Two arterial phase CT images in axial plane show an ill-defined hypovascular mass at head of pancreas (white arrow, B) which causes main pancreatic duct dilatation (white arrowheads, C). Loss of fat plane between the mass and 2nd part of duodenum is also noted, suggestive of local invasion. D: Portal venous phase CT images in coronal plane shows CBD (black arrow) and intrahepatic duct [IHD] dilatation (black arrowhead).

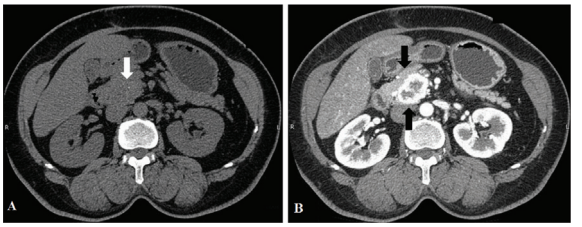

**Figure 2.** A 49-year-old woman, history of Von Hippel-Lindau with pheochromocytoma of right adrenal gland and non-benign pancreatic neuroendocrine tumor. A: Non-contrast CT image in axial plane shows a calcific spot at head of pancreas (white arrow). B: Pancreatic phase CT image in axial plane shows a well-defined heterogeneous hypervascular mass at pancreatic head (black arrows). Neither adjacent organ invasion nor main pancreatic duct dilatation is seen. Pathological diagnosis revealed tumor >2 cm in size, corresponding with criteria diagnosis of nPET.

defined margin, presence of main pancreatic duct dilatation, presence of CBD dilatation, presence of liver metastasis, and tumor-to-pancreatic contrasts were also high sensitivity, specificity, PPV, and NPV values as summarized in Table 5.

## Discussion

Accurate differentiation between PAC and nPET is crucial for appropriate treatment planning. Although, surgical management is the only cure, about 75% of PAC patients have unresectable disease at presentation[3].

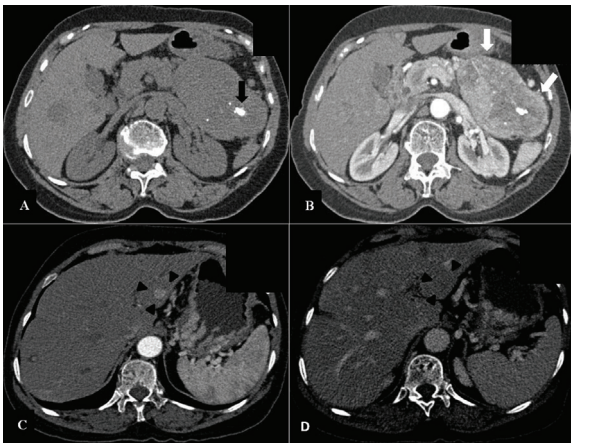

**Figure 3.** A 65-year-old female with non-benign pancreatic neuroendocrine tumor. A: Non-contrast CT image in axial plane shows a huge mass at pancreatic tail with internal calcification (black arrow). B: Arterial phase CT image in axial plane shows a well-defined heterogeneous hypervascular mass (white arrows) at pancreatic tail with internal calcification and necrosis. No main pancreatic duct dilatation is noted. C, D: Arterial and portal venous phases CT images in axial plane show a rather well-defined arterial enhancing lesion with faint wash out on portal venous phase at hepatic segment III (arrowheads), suggestive of liver metastasis. Pathologic diagnosis revealed tumor size of 11x10x6.5 cm, presence of vascular invasion and presence of liver metastasis, compatible with nPET.

**Table 4.** Tumor attenuation values and tumor-to-pancreas contrast of PAC and nPET

| | PAC (n = 49) | nPET (n = 18) | *p*-value* |
|---|---|---|---|
| Tumor attenuation (HU), mean ± SD | | | |
| Non-contrast | 36.3±6.3 | 40.7±9.3 | 0.028† |
| Arterial | 65.8±19.5 | 125.8±55.5 | 0.003† |
| Pancreatic | 66.3±18.2 | 98.0±52.1 | 0.248 |
| Portal venous | 81.0±22.3 | 109.9±22.9 | <0.001† |
| Delayed | 83.6±17.9 | 91.5±20.5 | 0.590 |
| Tumor-to-pancreas contrast, median (range) | | | |
| Non-contrast | -3.0 (-21.0 to 20.0) | 6.0 (-20.0 to 26.0) | 0.182 |
| Arterial | -40.5 (-111.0 to 18.0) | -5.0 (-51.0 to 134.0) | <0.001† |
| Pancreatic | -35.0 (-95.0 to 9.0) | -4.0 (-57.0 to 60.0) | 0.076 |
| Portal venous | -28.0 (-111.0 to 26.0) | 13.0 (-31.0 to 66.0) | <0.001† |
| Delayed | 3.0 (-45.0 to 27.0) | 25.5 (23.0 to 28.0) | 0.059 |

nPET = non-benign pancreatic neuroendocrine tumor; PAC = pancreatic adenocarcinoma

* Mann-Whitney test

† Statistically significant

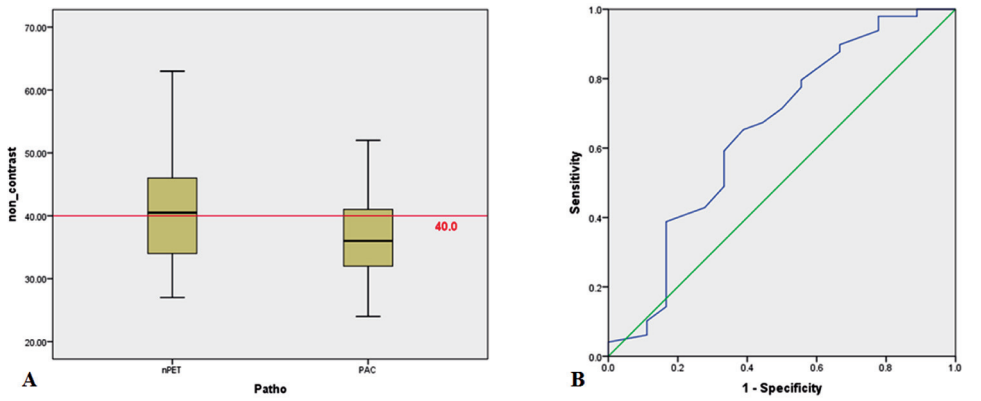


**Figure 4.** A: Box plot shows tumor attenuation on non-contrast phase (HU) in two groups: PAC and nPET. Red line indicates optimal cutoff value; black lines in boxes, median tumor attenuation (HU). B: Graph shows ROC curve for optimal cutoff value of tumor attenuation on non-contrast phase (HU) for differentiating PAC from nPET. Cutoff value is 40 HU (sensitivity 71.4%, specificity 50.0%, AUC 0.650).

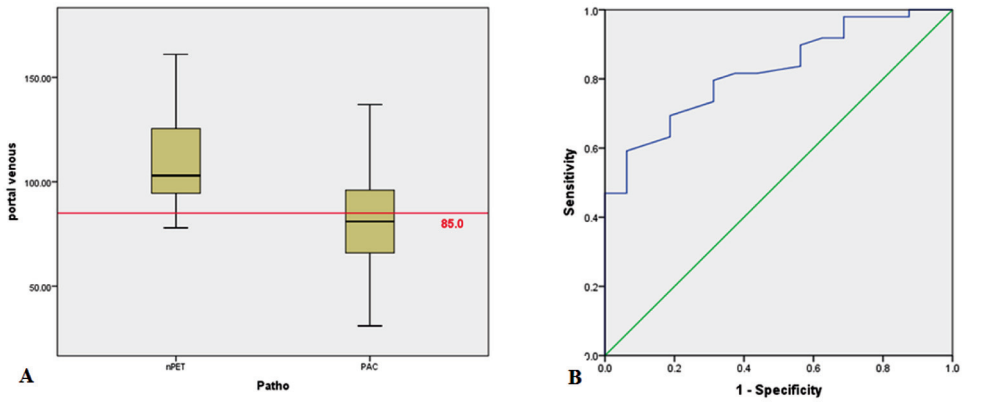


**Figure 5.** A: Box plot shows tumor attenuation on portal venous phase (HU) in two groups: PAC and nPET. Red line indicates optimal cutoff value; black lines in boxes, median tumor attenuation (HU). B: Graph shows ROC curve for optimal cutoff value of tumor attenuation on portal venous phase (HU) for differentiating PAC from nPET. Cutoff value is 85.0 HU (sensitivity 59.2%, specificity 93.7%, AUC 0.823).

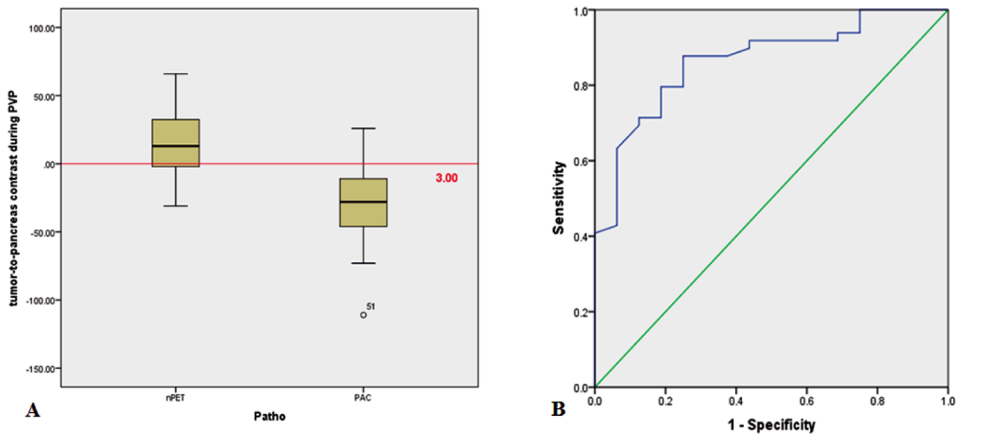


**Figure 6.** A: Box plot shows tumor-to-pancreas contrast during portal venous phase (HU) in two groups: PAC and nPET. Red line indicates optimal cutoff value; median tumor attenuation (HU). B: Graph shows ROC curve for optimal cutoff value of tumor-to-pancreas contrast during portal venous phase (HU) for PAC from nPET. Cutoff value is 3 HU (sensitivity 87.8%, specificity 75.0%, AUC 0.865).

**Table 5.** Statistical analysis of significant CT findings in difference of PAC and nPET

| CT findings | Sensitivity (95% CI) | Specificity (95% CI) | PPV (95% CI) | NPV (95% CI) |
|---|---|---|---|---|
| Head/uncinat/neck in location | 81.6 (68.0 to 91.2) | 61.1 (35.8 to 82.7) | 85.1 (75.9 to 91.2) | 55.0 (37.9 to 71.0) |
| An ill-defined margin | 95.9 (86.0 to 99.5) | 61.1 (35.8 to 82.7) | 87.0 (79.0 to 92.3) | 84.6 (57.4 to 95.7) |
| Absence of calcification | 83.7 (70.3 to 92.7) | 55.6 (30.8 to 78.5) | 83.7 (75.1 to 89.7) | 55.6 (37.0 to 72.7) |
| Hypo/isovascularity | 93.9 (83.1 to 98.7) | 77.8 (52.4 to 93.6) | 92.0 (82.9 to 96.5) | 82.4 (60.3 to 93.5) |
| Presence of main pancreatic duct dilatation | 77.6 (63.4 to 88.2) | 77.8 (52.4 to 93.6) | 90.5 (79.8 to 95.8) | 56.0 (41.7 to 69.4) |
| Presence of CBD dilatation | 73.5 (58.9 to 85.1) | 88.9 (65.3 to 98.6) | 94.7 (82.8 to 98.5) | 55.2 (42.9 to 66.9) |
| Absence of liver metastasis | 87.8 (75.2 to 95.4) | 66.7 (41.0 to 86.7) | 87.8 (78.7 to 93.3) | 66.7 (46.9 to 81.9) |
| Presence of adjacent organs invasion | 51.0 (36.3 to 65.6) | 83.3 (58.6 to 96.4) | 89.3 (74.1 to 96.0) | 38.5 (30.5 to 47.1) |
| Presence of intraabdominal lymphadenopathies | 75.5 (61.1 to 86.7) | 61.1 (35.8 to 82.7) | 84.1 (74.4 to 90.6) | 47.8 (33.2 to 62.9) |
| Tumor attenuation | | | | |
| On non-contrast phase <40 HU | 67.3 (52.5 to 80.1) | 55.6 (30.8 to 78.5) | 80.5 (70.4 to 87.8) | 38.5 (26.0 to 52.7) |
| On portal venous phase <85 HU | 55.1 (40.2 to 69.3) | 93.8 (69.8 to 99.8) | 96.4 (79.9 to 00.5) | 40.5 (32.8 to 48.8) |
| Tumor-to-pancreas contrast | | | | |
| During portal venous phase <3 HU | 87.8 (75.2 to 95.4) | 75.0 (47.6 to 92.7) | 91.5 (82.1 to 96.2) | 66.7 (47.3 to 81.7) |

CBD = common bile duct; CT = computed tomography; nPET = non-benign pancreatic neuroendocrine tumor; NPV = negative predictive value; PAC = pancreatic adenocarcinoma; PPV = positive predictive value

Thus, supportive treatment is the main therapeutic management in most patients with PAC. On the other hand, nPET shows overall better prognosis despite its non-benign behavior, less aggressive behavior, a higher resectability rate and better response to chemotherapy while it is a non-functioning tumor, as compared to PAC[12]. Tissue diagnosis, including Endoscopic Ultrasound-Guided Fine Needle Aspiration [EUS-FNA], transabdominal biopsy, and surgery are invasive and may provide procedure-related complications[13-15]. For these reasons, non-invasive imaging such as contrast-enhanced CT and magnetic resonance imaging [MRI], are preferred modalities for differentiating PAC from nPET.

It is well known that most patients with PAC are 60 to 80 years of age, and males are affected twice as frequently as females. For PET, most patients are 51 to 57 years at presentation[3]. In the present study, patient age also showed a statistically significant difference between PAC and nPET, which higher mean age was favored in PAC group (mean age of PAC and nPET were 64.5 and 54.9 years). However, no sexual predilection was demonstrated in PAC group in the present study.

As many as 10% to 15% of PET are associated with inherited syndrome such as multiple endocrine neoplasia type I [MEN-1], von Hippel-Lindau [VHL], neurofibromatosis I [NF-1], or tuberous sclerosis complex [TSC][16], but only one patient in nPET group or 5.6% of all nPETs in the present was associated with VHL. This may due to small number of nPET in this present study.

Although serum CA 19-9 is a reliable test for pancreatic cancer detection, only elevated CA 19-9 level cannot discriminate between benign and malignant disease and cannot differentiate type of the pancreatic cancer[17]. However, the present showed that patients with PAC had higher serum CA 19-9 level than nPET group ($p$ = 0.012), significantly. The median value (range) of serum CA 19-9 level in patients with PAC and nPET were 494.7 (0.6 to 44829.0) U/ml and 22.3 (1.2 to 175.6) U/ml, respectively, which the reference range of Siriraj Hospital is 0 to 39 U/ml.

Regarding the location of the tumor, PAC is typically located at pancreatic head, while location of PET is variable by its subgroups[3], concordant with the present's findings. In the present study, head, uncinate process, or neck of pancreas in location, was significantly more frequently observed in PAC than nPET as follows, almost of PACs (81.6%) were located in the head/uncinate/neck of pancreas, whereas most of nPETs (61.1%) were located in the body/tail/diffused.

In the present study, PAC frequently appeared as an ill-defined mass (95.9%), which was a significant difference from the sharpness of nPET (61.1%). This may indicate a relatively strong desmoplastic reaction in microscopic findings in PAC[18,19].

Vascularity of the tumor is thought to be the main criteria for differentiation between PAC and nPET because of difference in their blood supply, which PAC often shows hypovascularity as opposed to the hyper-vascularity in nPET[3]. Nevertheless, isoattenuating PAC can be seen as frequently as 10% in the study by Prokesch et al[20]. As shown in previous studies, 93.9%

of patients with PAC had hypo or isovascular tumor, while 77.8% of nPETs were hypervascular. The finding was also similar to this study, which 77.8% of patients with nPET had hypervascularity, while 93.9% of patients with PAC had hypo or isovascularity. For these reasons, all the tumor attenuation values during non-contrast, arterial, and portovenous phases, and tumor-to-pancreas contrast during arterial and portal venous phases, tended to be lower in PAC.

As mentioned above, almost all PACS are located at head of pancreas resulting in pressure effect to main pancreatic duct [MPD] and CBD. Therefore, upstream dilatation of both MPD and CBD is common in PAC[3]. This conforms to the results in this present study. The present study revealed that there was a statistically significant difference in bile duct dilatation between PAC and nPET, which approximately 77.6% and 73.5% of PACs associated with MPD and CBD dilatation, while only 22.2% and 5.6% of nPETs did, respectively.

The liver is the most common site for distant metastasis in both PAC and PET, particularly malignant PET[3,4]. In the present study, nPET had a significant tendency to metastasize to liver more than PAC, as many as 66.7% of nPETs showed liver metastasis, conversely, only 12.2% of PACs metastasized to liver. Based on vascularity of their primary tumor, the liver metastasis from PAC generally has hypovascularity but from nPET has hypervascularity[4,21].

The route of local spread of disease was primarily determined by location of the tumor, which tumor of head and uncinate process of pancreas, such as PAC, could spread to adjacent organs via perineural invasion[22]. The previous study reported that 53% to 100% of PACs showed perineural spreading. However, local invasion may be also seen in nPET[6]. In the present study, presence of adjacent organ invasion was a significant feature favoring PAC as 51.0% of PACs showed local invasion but nPET did only at 16.7%.

Although both PAC and PET are associated with peripancreatic lymph node enlargement[3,4,6], intra-abdominal lymphadenopathies were presented in PAC group more than nPET, with statistical significance. The authors found that 75.5% of PACs and only 38.9% of PETs demonstrated lymphadenopathies in the present study.

Regarding appearance, pattern enhancement, presence of necrosis, adjacent vessel invasion, and peritoneal metastasis, the present study revealed that these CT features were not significant difference between PAC and nPET. Low et al[3] mentioned about the major imaging features that aid to differentiate PAC from PET, which were 1) PAC is generally hypovascular, whereas PET is a hypervascularity tumor, 2) calcification is less frequent in PAC than PET, 3) vascular invasion is favoring PAC, 4) ductal dilatation usually shows in PAC, and 5) PAC often lacks central necrosis or cystic degeneration. In the present study, only vascular involvement and presence of necrosis did not agreed with that article. However, a study conducted by Gallotti et al[6], the presence of cystic degeneration and vascular invasion were some features that correlated to nPET. This phenomenon may be attributed to non-significant differentiation in central necrosis and adjacent vessel invasion between PAC and nPET in the present study.

The present study demonstrated that overall CT diagnostic accuracy compared with pathologic diagnosis in differentiating between PAC and nPET was 92.5%, with the sensitivity and specificity were 94.1% and 83.3%, respectively.

It is important to note that the present study had several limitations. First, the sample size was small. The authors propose that the present's findings be reproduced in an independent cohort. Second, because of the nature of the retrospective study, it may have introduced inherent selection bias such as the presence of risk factors and clinical presentation that were not controlled. This may have impaired the comparability of the two groups. Third, the CT protocols and machines used in our study were not uniform because of Siriraj Hospital is a tertiary referral hospital and designation in CT protocol is mainly dependent on clinical presentation and radiation dose consideration. Then arterial/pancreatic phases were not performed in every patient. Finally, both reviewers realized that all cases in the present were either PAC or nPET, which may affect the accuracy of CT diagnosis.

## Conclusion

Abdominal contrast-enhanced CT is the reliable method to differentiate between PAC and nPET. An ill-defined margin, hypo/isovascularity, and absence of liver metastasis were predictive findings for PAC and may help differentiate it from nPET.

## What is already known on this topic?

Differentiation of PAC from PET based on its typical features on CT imaging could be made by considering 1) pattern enhancement, 2) presence of calcification, 3) vascular involvement, 4) ductal involvement, and 5) presence of central necrosis and cystic degeneration. However, differentiating between

PAC and nPET on the basis of CT imaging is not well known.

## What this study adds?

In the present study, tumor demarcation, pattern enhancement, and liver metastasis, are CT features that aid to differentiating between PAC and nPET, which an ill-defined margin, hypo/isovascularity, and absence of liver metastasis were more indicative of PAC than nPET.


## Acknowledgement

The authors would like to thank Suthipol Udompunturak for the statistical analysis.


## Potential conflicts of interest

The authors declare no conflict of interest.

## References


1. Siegel R, Ma J, Zou Z, Jemal A. Cancer statistics, 2014. CA Cancer J Clin 2014;64:9-29.
2. National Cancer Institute, Department of Medical Services, Ministry of Public Heath, Thailand. Hospital-based cancer Registry, Annual report 2014. Bangkok: National Cancer Institute; 2016.
3. Low G, Panu A, Millo N, Leen E. Multimodality imaging of neoplastic and nonneoplastic solid lesions of the pancreas. Radiographics 2011;31: 993-1015.
4. Noone TC, Hosey J, Firat Z, Semelka RC. Imaging and localization of islet-cell tumours of the pancreas on CT and MRI. Best Pract Res Clin Endocrinol Metab 2005;19:195-211.
5. Tan EH, Tan CH. Imaging of gastroenteropancreatic neuroendocrine tumors. World J Clin Oncol 2011; 2:28-43.
6. Gallotti A, Johnston RP, Bonaffini PA, Ingkakul T, Deshpande V, Fernandez-del Castillo C, et al. Incidental neuroendocrine tumors of the pancreas: MDCT findings and features of malignancy. AJR Am J Roentgenol 2013;200:355-62.
7. Winter TC, Ager JD, Nghiem HV, Hill RS, Harrison SD, Freeny PC. Upper gastrointestinal tract and abdomen: water as an orally administered contrast agent for helical CT. Radiology 1996;201:365-70.
8. Vargas R, Nino-Murcia M, Trueblood W, Jeffrey RB Jr. MDCT in Pancreatic adenocarcinoma: prediction of vascular invasion and resectability using a multiphasic technique with curved planar reformations. AJR Am J Roentgenol 2004;182: 419-25.
9. Hough TJ, Raptopoulos V, Siewert B, Matthews JB. Teardrop superior mesenteric vein: CT sign for unresectable carcinoma of the pancreas. AJR Am J Roentgenol 1999;173:1509-12.
10. Roche CJ, Hughes ML, Garvey CJ, Campbell F, White DA, Jones L, et al. CT and pathologic assessment of prospective nodal staging in patients with ductal adenocarcinoma of the head of the pancreas. AJR Am J Roentgenol 2003;180:475-80.
11. Landis JR, Koch GG. The measurement of observer agreement for categorical data. Biometrics 1977; 33:159-74.
12. Liang H, Wang P, Wang XN, Wang JC, Hao XS. Management of nonfunctioning islet cell tumors. World J Gastroenterol 2004;10:1806-9.
13. Early DS, Acosta RD, Chandrasekhara V, Chathadi KV, Decker GA, Evans JA, et al. Adverse events associated with EUS and EUS with FNA. Gastrointest Endosc 2013;77:839-43.
14. Tyng CJ, Almeida MF, Barbosa PN, Bitencourt AG, Berg JA, Maciel MS, et al. Computed tomography-guided percutaneous core needle biopsy in pancreatic tumor diagnosis. World J Gastroenterol 2015;21:3579-86.
15. Ho CK, Kleeff J, Friess H, Buchler MW. Complications of pancreatic surgery. HPB (Oxford) 2005;7:99-108.
16. Oberg K. Pancreatic endocrine tumors. Semin Oncol 2010;37:594-618.
17. Mann DV, Edwards R, Ho S, Lau WY, Glazer G. Elevated tumour marker CA19-9: clinical interpretation and influence of obstructive jaundice. Eur J Surg Oncol 2000;26:474-9.
18. Hruban RH, Klimstra DS. Adenocarcinoma of the pancreas. Semin Diagn Pathol 2014;31:443-51.
19. Hruban RH, Fukushima N. Pancreatic adenocarcinoma: update on the surgical pathology of carcinomas of ductal origin and PanINs. Mod Pathol 2007;20(Suppl 1):S61-70.
20. Prokesch RW, Chow LC, Beaulieu CF, Bammer R, Jeffrey RB Jr. Isoattenuating pancreatic adenocarcinoma at multi-detector row CT: secondary signs. Radiology 2002;224:764-8.
21. Danet IM, Semelka RC, Nagase LL, Woosely JT, Leonardou P, Armao D. Liver metastases from pancreatic adenocarcinoma: MR imaging characteristics. J Magn Reson Imaging 2003;18:181-8.
22. Pietryga JA, Morgan DE. Imaging preoperatively for pancreatic adenocarcinoma. J Gastrointest Oncol 2015;6:343-57.